Contents lists available at ScienceDirect

Arabian Journal of Chemistry

journal homepage: www.ksu.edu.sa

Original article

Phytochemical profiles and protein glycation inhibitory activities of three oak species

Su Hui Seong [a], Bo-Ram Kim [a], Seahee Han [b], Jin-Ho Kim [a], Sua Im [a], Tae-Su Kim [a], Chan Seo [a], Ha-Nul Lee [a], Jung Eun Kim [a], Ji Min Jung [a], Myoung Lae Cho [c], Kyung-Min Choi [d], Jin-Woo Jeong [a,*]

[a] Division of Natural Products Research, Honam National Institute of Biological Resources, Mokpo 58762, Republic of Korea
[b] Division of Botany, Honam National Institute of Biological Resources, Mokpo 58762, Republic of Korea
[c] Division of Research Management, Honam National Institute of Biological Resources, Mokpo 58762, Republic of Korea
[d] Department of Integrative Bioresources, Honam National Institute of Biological Resources, Mokpo 58762, Republic of Korea

ARTICLE INFO

Keywords:
Quercus
Oak
Anti-glycation
Methylglyoxal-adduct
Ellagitannin
Advanced glycation end products
UPLC-Q-TOF-MS

ABSTRACT

The Quercus genus (oaks) comprises valuable plant resources that are used in many fields, including cosmetics, foods, and pharmaceuticals. Nonetheless, overall chemical profiling and anti-glycation component identification have not been thoroughly performed. In the present study, 70 % ethanolic and water extracts from three oak species (*Quercus dentata, Q. serrata, and Q. aliena)* showed antioxidant and anti-glycation potential. Thus, the components of the three oak species were profiled using ultra-performance liquid chromatography coupled with electrospray ionization and quadrupole time-of-flight mass spectrometry. The analysis showed that phenolic acids, ellagitannins, ellagic acid, procyanidin, and flavonoid (quercetin, myricetin, kaempferol, isorhamnetin, and taxifolin) glycosides are the main phenolic compounds. Based on the fluorescence assay, they act as strong inhibitors of non-enzymatic advanced glycation end-products (AGEs) formation in the bovine serum albumin (BSA) and skin proteins (collagen and elastin). Furthermore, mass fragmentation analysis demonstrated that ellagitannin, procyanidin B1 and flavonoid glycosides effectively trapped methylglyoxal (MGO), a reactive carbonyl intermediate and an important precursor of AGEs, to generate mono-, di-, or tri-MGO. Collectively, ellagic acid, ellagitannins, procyanidin B1, and flavonoid glycosides, the main active ingredients of three oak species (*Q. dentata, Q. serrata,* and *Q. aliena)*, may be employed as lead structures in the development of functional foods or drugs to prevent diseases caused by aging and excessive sugar consumption.

1. Introduction

The Maillard reaction (MR) is a complex series of chemical reactions between reducing sugars and proteins that leads to protein browning, fluorescence, and crosslinking (Jia et al., 2023; Mazumder et al., 2019). Advanced glycation end products (AGEs), which are produced in the later stages of the MR, can accumulate in long-lived tissue proteins, such as collagen and lens crystallin, and may play a role in the development of metabolic illnesses such as diabetes, diabetic complications, and neuronal disorders (Liu et al., 2022). Reducing sugars, including glucose and fructose, react non-enzymatically with the H_2N-protein through a three-step non-enzymatic protein glycation process. The carbonyl group (–COOH) of glucose combines with the H_2N-protein to form Schiff bases, followed by a stable Amadori rearrangement product (ARP) (Grillo and Colombatto, 2008). These ARPs then undergo various irreversible dehydration and rearrangement reactions leading to the formation of reactive carbonyl compounds (RCCs) such as methylglyoxal (MGO). Subsequently, RCCs react with H_2N, guanidine, and SH groups in proteins, ultimately generating irreversible AGEs (Chaudhuri et al., 2018; Choei et al., 2004). Recent studies have suggested that AGEs derived from α-hydroxyaldehyde, such as glyceraldehyde (GLAD) and glycoaldehyde, show stronger neurotoxicity and stronger promotion of radical formation than AGEs derived from glucose (Takeuchi et al., 2000). In addition, the browning activity due to α-hydroxyaldehyde was approximately 2000 times greater than glucose in the early stage of the MR. These GLADs are formed from GLAD-3-phosphate, an intermediate of glycolysis, or fructose through the polyol pathway or food intake (Choei et al., 2004). The identification of active substances that can

* Corresponding author.
E-mail address: jwjeong@hnibr.re.kr (J.-W. Jeong).

https://doi.org/10.1016/j.arabjc.2024.106039
Received 14 May 2024; Accepted 30 October 2024
Available online 7 November 2024

reduce carbonyl stress (accumulation of RCCs) and prevent AGE formation is thus vital.

The *Quercus* genus comprises tree species commonly named oaks and belongs to the Fagaceae family. The genus contains more than 450 species distributed worldwide. Oaks are used as natural antioxidants in food preservation and play an important role in wine maturation in oak barrels (Morales, 2021). Several studies have demonstrated that oak extracts possess antioxidant, antiseptic, antibacterial, antifungal, anti-acne, anti-inflammatory, antibiofilm, and anti-diabetic properties (Burlacu et al., 2020; Othón-Díaz et al., 2023; Taib et al., 2020). Particularly, *Quercus mongolica* and its constituents (ellagic acid and kaempferol derivatives) showed inhibitory activities against AGE formation and digestive enzymes including α-glucosidase and α-amylase (Yin et al., 2018). The bioactive components of oaks include polar or moderately polar compounds (*e.g.*, ellagic acid, tannins, flavonoids, flavonoid glycosides, and phenolic acids), and nonpolar compounds (*e.g.*, terpenoids, fatty acids, and sterols) (Morales, 2021). However, the overall phytochemical profile and identification of the anti-glycation compounds of *Quercus dentata* Thunb, *Quercus serrata* Murray, and *Quercus aliena* Blume have not yet been completed. This study aimed to address this gap in our knowledge by profiling the constituents of the leaves, stems, and fruits from these oak species using ultra-performance liquid chromatography coupled with electrospray ionization quadrupole time-of-flight mass spectrometry (UPLC-ESI-Q-TOF-MS); furthermore, we aimed at clarifying their antioxidant and protein (serum albumin, collagen, and elastin) glycation inhibitory potential *in vitro*.

2. Materials and methods

2.1. Chemicals and reagents

In this study, 2,2′-azino-bis(3-ethylbenzothiazoline-6-sulfonic acid) diammonium salt (ABTS), bovine serum albumin (BSA), monosaccharides, and methylglyoxal solution (40 %, *v/v*), thioflavin T (ThT) and standards including aminoguanidine HCl (AG) and L-ascorbic acid were all purchased from Sigma-Aldrich (St. Louis, MO, USA). 1,1-Diphenyl-2-picrylhydrazyl radical (DPPH) was purchased from Santa Cruz Biotechnology (Santa Cruz, CA, USA). All the solvents used for instrumental analysis were purchased from Merck (Darmstadt, Germany).

2.2. Plant materials

Quercus dentata Thunb and *Q. serrata* Murray were collected from the Aphaedo and Chupodo Islands (Shinan-gun, Jeollanam-do, Republic of Korea), respectively, in July 2021. *Quercus aliena* Blume was collected from Jindo Island (Jindo-gun, Jeollanam-do, Republic of Korea) in August 2021. The plants were authenticated by Dr. S Han of the Honam National Institute of Biological Resources (voucher no. shan2021-16 for *Q. dentata*, shan2021-48 for *Q. serrata*, and shan2021-95 for *Q. aliena*). The 70 % ethanol (EtOH) and aqueous extracts from the different parts (leaves, fruits, twigs) of three oak species were received from the Bank of Bioresources from Island and Coast (BOBIC), Republic of Korea (registered no. HNIBR NP40, NP42, NP154, and NP156 for *Q. dentata*; NP145, NP147, NP148, NP150, NP169, and NP171 for *Q. serrata*; and NP259, NP261, NP262, NP264, NP289, and NP291 for *Q. aliena*).

2.3. UPLC-ESI-Q-TOF-MS analysis

Separation of 70 % EtOH and the aqueous extract from the different organs of the three oak species studied was performed using a C_{18} column (1.7 μm, 2.1 × 100 mm) and Waters ACQUITY UPLC I-Class Plus System (Waters Corporation, Milford, MA, USA). The gradient mobile phase consisted of MS-grade water (A) and MS-grade acetonitrile (ACN) (B), with 0.1 % MS-grade HCOOH: 0–10 min, B 2 % to 11 %; 10–12 min, B 11 to 11 %; 12–14 min, B 11 to 20 %; 14–20 min, B 20 to 23 %; 20–35 min, B 23 to 50. The column was heated to 30 °C, and the sample injection volume was 1 μL (0.2 mL/min flow rate). Mass analysis was conducted using Q-TOF-MS (Xevo G2-XS, Waters Corporation, Milford, MA, USA) with a mass range of 50–1500 Da in the negative ion mode, at 40 V cone voltage, and 350 ℃ desolvation temperature; further, 0.5 mM HCOONa and 0.2 ng/mL [Leu5]-enkephalin were used for mass calibration and correction.

2.4. Antioxidant assay

The radical-scavenging activities extracted from the different organs of the three oak species under study were assessed using the ABTS and DPPH radical scavenging method, as previously described, with L-ascorbic acid as the standard (Dudonné et al., 2009).

2.5. Protein glycation inhibitory assays

The BSA glycation inhibitory assay was conducted as previously described (Seong et al., 2021; Vinson and Howard, 1996). To formulate the glucose/fructose-induced AGEs reaction solution (ARS), 0.01 g/mL BSA in 0.05 M sodium phosphate buffer (pH 7.4) was added to 0.4 M monosaccharides, which include D-(−)-fructose and D-(+)-glucose, and 0.02 % NaN_3. Various doses of extracts from the three oak species and their constituents were added to the ARS, and the mixtures were incubated at 37 °C for one week. To formulate the BSA-fructose model ($gBSA^{fru}$), 0.01 g/mL BSA in 0.05 M sodium phosphate buffer (pH 7.4) was added to 0.4 M D-(−)-fructose and 0.02 % NaN_3 (Yamaguchi et al., 2000). Various doses of AG and oak-derived constituents were added to the $gBSA^{fru}$, and the mixtures were incubated at 50 °C for 72 h. A microplate reader (Biotek, Winooski, VT, USA) was used to measure AGEs generation at excitation and emission wavelengths of 350 and 450 nm, respectively. Glycation of collagen and elastin was induced by glyceraldehyde, and the anti-glycation activities of the test compounds were determined following manufacturer instructions (Cosmo Bio Co., Ltd., Carlsbad, USA). AG was used as a reference substance for the protein glycation assays (Thornalley, 2003).

2.6. Fluorescence assay for AGEs and protein oxidation products

The specific AGEs produced in the $gBSA^{fru}$ model were measured by fluorescence at their characteristic excitation and emission wavelengths: argpyrimidine (APN) at 320 and 380 nm, crossline (CL) at 380 and 440 nm, pentosidine (PEN) at 335 and 385 nm, and vesperlysine (VL) at 366 and 442 nm (Awasthi and Saraswathi, 2016). Additionally, the protein oxidation products generated in the $gBSA^{fru}$ model were also measured by fluorescence at their characteristic excitation and emission wavelengths: dityrosine (di-Tyr) at 330 and 415 nm, N′-formyl kynurenine (NFK) at 325 and 434 nm, and kynurenine at 365 and 480 nm (Zhang et al., 2022). Fluorescence from the glycated samples were measured by scanning with excitation wavelengths at 335 and 370 nm and emission wavelengths in the range of 350–600 nm.

2.7. β-Amyloid protein aggregation assay

Glycated protein ($gBSA^{fru}$) was incubated with 20 μg/mL ThT solution at 37 °C for 1 h (Bouma et al., 2003). Subsequently, the fluorescence spectra of the reaction mixture were measured by scanning with an excitation wavelength at 435 nm and emission wavelengths in the range of 460–600 nm, with intensity recorded at 485 nm for the calculation of the inhibition rate.

2.8. Analysis of MGO adducts of the components from the three oak species under physiological conditions

MGO was mixed with components from different parts of the three oak species at a molar ratio of 3:1 in 1 × phosphate-buffered saline (PBS)

(Ni et al., 2021). After 24 h of incubation at 37 °C, the compound–MGO reaction solution was filtered using a 0.2 μm pore syringe and the filtrate was analyzed a 5-μm reversed-phase analytical column (250 × 4.6 mm, C_{18} silica) and high-performance liquid chromatography (HPLC) (Ultimate™ 3000, ThermoScientific, Pittsburgh, PA, USA). The gradient mobile phase consisted of MS-grade water (A) and MS-grade ACN (B), with 0.1 % MS-grade HCOOH: 0–65 min, B 5 %–25 %. The column was heated to 30 °C, and the sample injection volume was 2.5 μ L (0.5 mL/min flow rate). MS conditions were the same as those mentioned in Section 2.3.

2.9. Statistical analysis

The 50 % effective and inhibitory concentrations (EC_{50} and IC_{50}, respectively; μg/mL or μM) obtained from dose/inhibition curves were expressed as means ± standard deviation (SD) obtained from three independent experiments.

3. Results

3.1. Antioxidant and anti-glycation potentials of the extracts from the three oak species

To determine the antioxidant and anti-glycation potentials of the three oak species studied herein, the $ABTS^{\cdot+}$ and DPPH radical-scavenging assay and the monosaccharide-induced BSA glycation assay were conducted with appropriate reference compounds (Fig. 1). Aqueous extracts of the different organs of the *Q. dentata*, *Q. serrata*, and *Q. aliena*, showed strong antioxidant activity, with more than 90 % $ABTS^{\cdot+}$ and DPPH radical-scavenging activity at 50 μg/mL. In addition, the 70 % ethanolic extracts of *Q. dentata* (leaves and twigs), *Q. serrata* (leaves, twigs, and fruits), and *Q. aliena* (leaves and twigs) showed strong antioxidant activity, similar to that of the aqueous extracts. However, the 70 % ethanolic extract of the *Q. aliena* fruit showed no activity at the tested concentrations. For the anti-glycation activity, all extracts, except for the 70 % ethanolic extract from the *Q. aliena* fruits, showed good inhibition against monosaccharide-induced AGE formation. Among them, the 70 % ethanolic and aqueous extracts derived from the *Q. aliena* twigs showed the strongest anti-glycation, with IC_{50} values of 7.06 and 7.49 μg/mL, respectively.

3.2. UPLC-ESI-Q-TOF-MS profiles of the three oak species

The chemical constituents of the leaves, twigs, and fruits from the three oak species (*Q. dentata, Q. serrata,* and *Q. aliena*) were analyzed using UPLC-ESI-Q-TOF-MS (Figs. 2–3 and Table 1). As a result, 47 phytochemicals—eleven phenolic acids (**1**–**11**), ten ellagitannins (**12**–**21**), ellagic acid (**22**), two catechins (**25, 26**), two B-type procyanidins (**23, 24**), five taxifolin derivatives (**27**–**29, 32, 36**), three myricetin derivative (**30, 31, 33**), six quercetin derivatives (**34, 35, 37, 39, 41, 43**), four kaempferol derivative (**38, 40, 44, 45**), one isorhamnetin derivative (**42**), and two liganas (**46** and **47**)—were detected in the negative ion mode of the MS and tentatively identified by interpreting the high-resolution mass spectra (fragmentation patterns obtained from high energy function).

According to the UPLC-ESI-Q-TOF-MS results, quinic acid (**1**), gallic acid (**2**), (+)-catechin (**25**), ellagitannins (**16**–**18**), ellagic acid (**22**), and flavonoid glycosides appeared to be common compounds in *Q. dentata, Q. serrata,* and *Q. aliena*. Interestingly, taxifolin (**36**) and its glycosides (**27**–**29**) were only detected in *Q. serrata* (Fig. 2B). Compared to that in other *Quercus* spp., the peak of quercitrin (**41**) was significantly higher in the UPLC-MS base peak intensity (BPI) chromatogram of the extracts from *Q. serrata* leaves (Fig. 2B). As shown in Fig. 2C, the galloylquinic acid (**3**), ellagitannins of the di-hexahydroxydiphenoyl (HHDP)-glucose structure (**12, 15, 17, 19**) and galloyl-di-HHDP-glucose structure (**21**) was relatively high in *Q. aliena* when compared with the values for the other oak species.

3.2.1. Identification of phenolic acids

Quinic acid (**1**) and its derivatives (**3**–**11**) in the three oak species were identified and deduced in accordance with the core-compound diagnostic ion at *m/z* 191.0559 (quinic acid) and fragmentation pattern. Compound **3** was identified as galloylquinic acid due to the loss of galloyl moiety (170 Da–H_2O). Compounds **4** and **6** were characterized as caffeoylquinic acids due to the loss of caffeoyl moiety (180 Da–H_2O). Similarly, compounds **5**, **7**, and **8** were characterized as coumaroylquinic acids due to the loss of coumaroyl moiety (164 Da–H_2O). Compounds **9**–**11** were identified as dicaffeoylquinic acids due to their

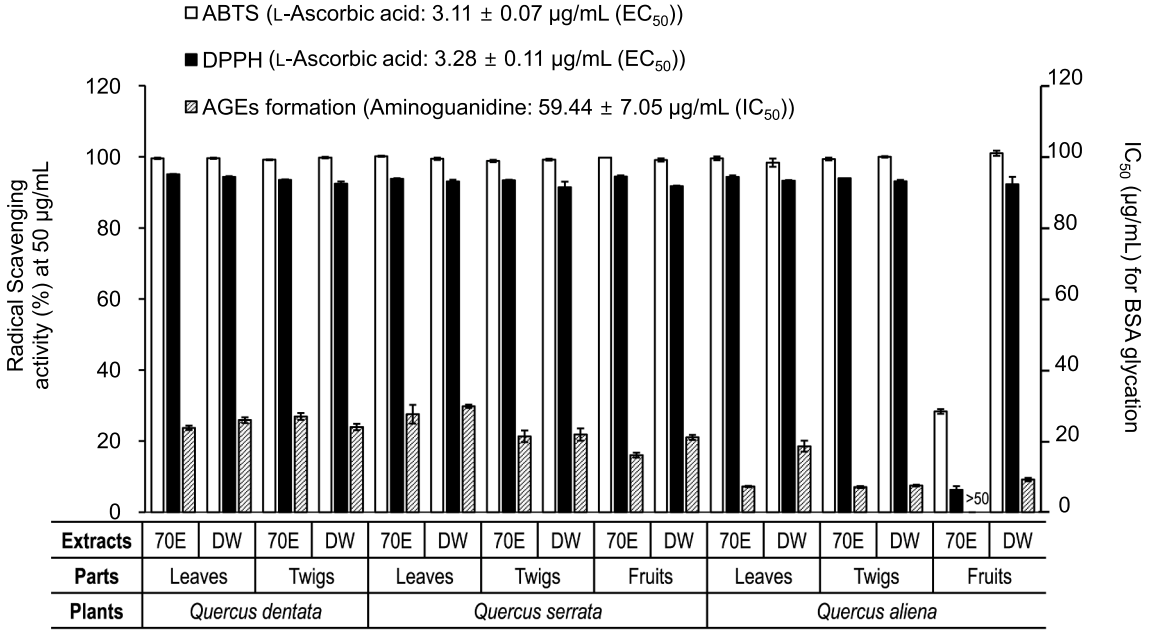

Fig. 1. Antioxidant and AGEs formation (BSA/monosaccharide system) inhibitory activities of 70% EtOH (70E) and water (DW) extracts from different parts of three oak species (*Quercus dentata, Q. serrata,* and *Q. aliena*).

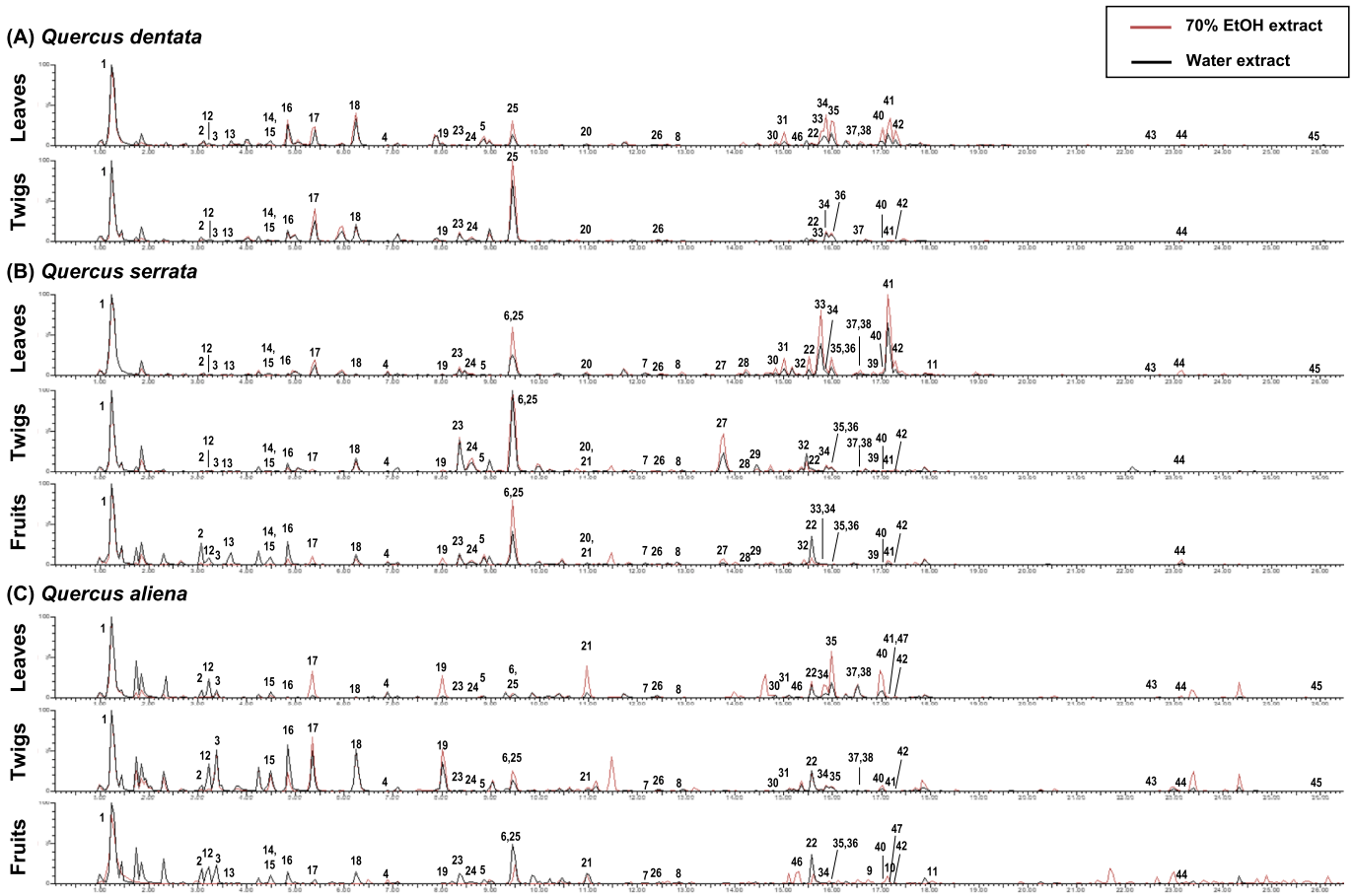

Fig. 2. The UPLC-MS base peak intensity (BPI) chromatogram of various extracts from *Quercus dentata* (A), *Q. serrata* (B), *and Q. aliena* (C).

common fragment ions at *m/z* 179.0353 [M-caffeoyl-quinic acid-H]$^-$. Compared with reference standards, compounds **2** and **4**–**11** were identified as gallic acid, neochlorogenic acid, 3-*O*-coumaroylquinic acid, chlorogenic acid, 5-*O*-coumaroylquinic acid, 4-*O*-coumaroylquinic acid, 3,4-dicaffeoylquinic acid, 3,5-dicaffeoylquinic acid, and 4,5-dicaffeoylquinic acid, respectively.

3.2.2. Identification of ellagitannin and ellagic acid

The ellagitannins (**12**–**21**) in the three oak species were identified and deduced in accordance with the core-compound diagnostic ion at *m/z* 300.9988 (ellagic acid). Compounds **12**, **15**, **17**, and **19** were characterized as di-HHDP-glucose structure type ellagitannins due to their common fragment ion at *m/z* 481.0636 [M-HHDP-H]$^-$. Compound **21** was identified as galloyl-di-HHDP-glucose structure type ellagitannin, casuarinin, due to their common fragment ion at *m/z* 633.0742 [M-HHDP-H]$^-$ and 783.0709 [M-galloyl-H]$^-$. Compounds **13** was characterized as vescavaloninic acid due to its doubly charged fragment ions (*m/z* 550.0341 [M-2H]$^{2-}$ and 528.0372 [M-H-COOH]$^{2-}$) and its daughter ions (*m/z* 631.0605 [M-valoneoyl-H, vescalin]$^-$, 1039.0681 [M-H_2O-COOH]$^-$ and 1083.0632 [M-H-H_2O]$^-$). Similarly, compounds **14** was characterized as castavaloninic acid due to its doubly charged fragment ions (*m/z* 550.0341 [M-2H]$^{2-}$ and 528.0372 [M-H-COOH]$^{2-}$) and its daughter ions (*m/z* 631.0605 [M-valoneoyl-H, castalin]$^-$ and 1057.0863 [M-COOH]$^-$). Compounds **16**, **18**, and **20** were characterized as HHDP-NHTP type ellagitannins due to their common fragment ion at *m/z* 631.0605 [M-HHDP-H]$^-$ and 613.0481 [M-HHDP-H_2O-H]$^-$. Compared with reference standard, compound **16** and **18** were identified as vescalagin and castalagin, respectively.

3.2.3. Identification of flavonoids

The flavonoids (**23**–**45**) in the three oak species were identified and deduced in accordance with the main aglycone diagnostic ions (catechin, taxifolin, myricetin, quercetin, kaempferol, isorhamnetin) as well as the fragmentation pattern. Compounds **23** and **24** were characterized as B-type procyanidins due to their diagnostic ion at *m/z* 289.0710 and fragmentation ion at *m/z* 407.0787, which resulted from *retro*-Diels-Alder (rDA) reaction and the loss of water. Compared with reference standard, compound **23** was identified as procyanidin B1. Taxifolin derivatives (**27**–**29** and **32**) were the major flavanonols in *Q. serrata* under investigation, according to their common fragment ion at *m/z* 285.0424. Compared with reference standard, compounds **27**, **29**, **32**, and **36** were identified as (2*R*,3*R*)-(+)-glucodistylin, (2*S*,3*S*)-(+)-glucodistylin, taxifolin-3′-O-glucopyranoside, and taxifolin, respectively. Myricetin derivatives (**33** and **33**) were the major flavanonols in *Q. dentata* under investigation, according to their common fragment ion at *m/z* 316.0212 (deprotonated myricetin). Compared with reference standard, compound **33** was identified myricitrin (myricetin-3-*O*-α-L-rhamnopyranoside). Quercetin derivatives (**34**, **35**, **37**, **39**, and **41**) were the common flavonols in *Quercus* species under investigation, according to their common fragment ions at *m/z* 301.0344 (quercetin) and 300.0285 (deprotonated quercetin). Compared with reference standard, compounds **34**, **35**, **37**, **39**, **41** and **43** were identified hyperoside, isoquercitrin, quercetin-3-*O*-α-L-arabinopyranoside, avicularin (quercetin-3-*O*-α-L-arabinofuranoside), quercitrin, and quercetin, respectively. Kaempferol derivatives (**38** and **40**) were the common flavonols in *Quercus* species under investigation, according to their common fragment ion at *m/z* 285.0329 (kaempferol). Compound **44** was identified due to the loss of coumaroyl moiety (164 Da–H_2O) and glucose (180 Da–H_2O). Compared with reference standards, compounds **38**, **40**, **44**,

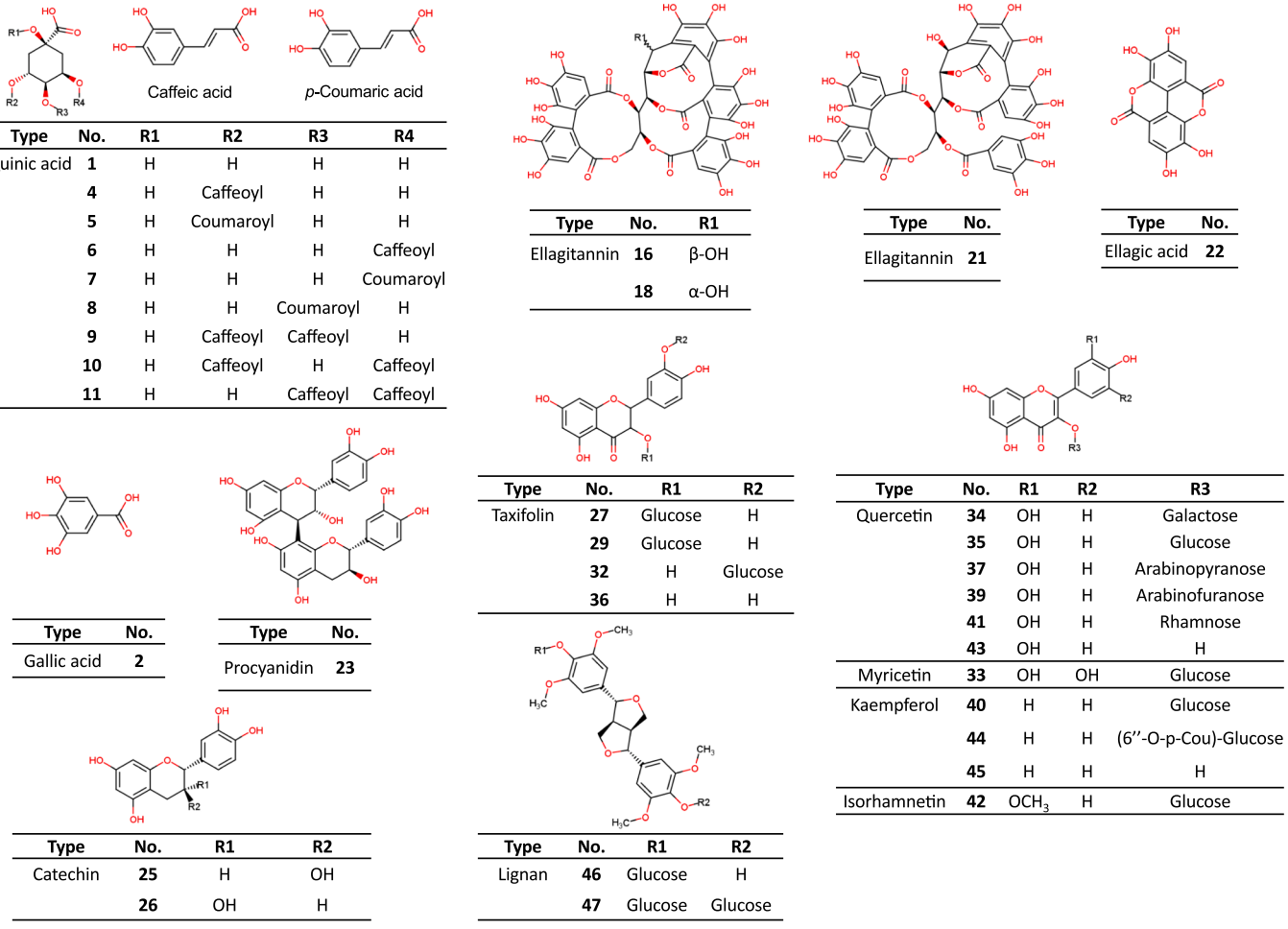

Type	No.	R1	R2	R3	R4
Quinic acid	1	H	H	H	H
	4	H	Caffeoyl	H	H
	5	H	Coumaroyl	H	H
	6	H	H	H	Caffeoyl
	7	H	H	H	Coumaroyl
	8	H	H	Coumaroyl	H
	9	H	Caffeoyl	Caffeoyl	H
	10	H	Caffeoyl	H	Caffeoyl
	11	H	H	Caffeoyl	Caffeoyl

Type	No.	R1
Ellagitannin	16	β-OH
	18	α-OH

Type	No.
Ellagitannin	21

Type	No.
Ellagic acid	22

Type	No.
Gallic acid	2

Type	No.
Procyanidin	23

Type	No.	R1	R2
Taxifolin	27	Glucose	H
	29	Glucose	H
	32	H	Glucose
	36	H	H

Type	No.	R1	R2
Catechin	25	H	OH
	26	OH	H

Type	No.	R1	R2
Lignan	46	Glucose	H
	47	Glucose	Glucose

Type	No.	R1	R2	R3
Quercetin	34	OH	H	Galactose
	35	OH	H	Glucose
	37	OH	H	Arabinopyranose
	39	OH	H	Arabinofuranose
	41	OH	H	Rhamnose
	43	OH	H	H
Myricetin	33	OH	OH	Glucose
Kaempferol	40	H	H	Glucose
	44	H	H	(6′′-O-p-Cou)-Glucose
	45	H	H	H
Isorhamnetin	42	OCH_3	H	Glucose

Fig. 3. Structures of the phytochemicals derived from *Quercus dentata, Q. serrata,* and *Q. aliena.*

and **45** were identified as kaempferol-*O*-hexoside, astragalin (kaempferol-3-*O*-glucopyranoside), tiliroside (6″-*O*-*trans*-*p*-coumaroylastragalin), and kaempferol, respectively. Compound **42** was identified as isorhamnetin-3-*O*-glucopyranoside due to its daughter ion at *m/z* 314.0422 (deprotonated isorhamnetin) and comparison with reference standard.

3.2.4. Identification of lignans

Syringaresinol derivatives (**46** and **47**) were detected in *Q. aliena* under investigation, according to their singly charged pseudo molecular ions (*m/z* 741.2628 for **46** and 579.2067 for **47**) and aglycone diagnostic ion (*m/z* 417.1578, syringaresinol). Compared with reference standards, compounds **46** and **47** were identified as syringaresinol-di-*O*-glucoside and syringaresinol-4-*O*-glucoside, respectively.

3.3. Inhibitory effects of the oak-derived components on protein glycation

Protein (BSA, collagen, and elastin) glycation inhibitory activities of the major components derived from the different organs of the three oak species studied herein were tested, and the results are shown in Fig. 4A. Castalagin (**18**) and ellagic acid (**22**) showed outstanding inhibitory activity against both glucose/fructose-induced BSA glycation and fructose-induced BSA glycation, followed by quercetin glycosides (**34**, **35**, and **41**) > taxifolin glycosides (**27** and **29**), taxifolin (**36**), procyanidin B1 (**23**) > caffeoylquinic acids (**4** and **6**), myricitrin (**33**), and isorhamnetin-3-*O*-glucoside (**42**) > (+)-catechin (**25**) > gallic acid (**2**). In addition to BSA glycation, skin protein glycation inhibition assays were performed using glyceraldehyde as a glycation inducer. In the collagen glycation assay, castalagin (**18**), procyanidin B1 (**23**), quercetin derivatives (**34**, **35**, and **41**), myricitrin (**33**), astragalin (**40**), and isorhamnetin-3-*O*-glucoside (**42**) showed almost 50 % inhibition of the collagen glycation at 0.2 mM. However, taxifolin (**36**) and its glycosides (**27** and **29**) showed weak inhibitory potentials, whereas the caffeoylquinic acids (**4** and **6**) showed no inhibitory activity. With the elastin glycation assay, ellagic acid (**22**) showed the strongest anti-glycation activity (78.26 % inhibition at 0.2 mM), followed by quercetin derivatives (**34**, **35**, and **41**), isorhamnetin-3-*O*-glucoside (**42**), and myricitrin (**33**). However, taxifolin (**36**) and its glycosides (**27** and **29**) showed weak inhibitory potential against skin protein glycation, whereas caffeoylquinic acids (**4** and **6**) showed no inhibitory activity at 0.2 mM. The anti-glycation efficacy of the three oak species is thus believed to be due to mainly the presence of ellagitannins and flavonoid glycosides.

3.4. Effects of the oak-derived components on fluorescent AGEs

The inhibitory effects of the oak-derived components on fluorescent AGEs in the gBSA^{fru} model were evaluated by measuring the fluorescence intensity of cross-linked AGEs (CL, PEN, and VL) and non-cross-linked AGEs (APN) (Perrone et al., 2020). As shown in Fig. 4B, both cross-linked AGEs and non-cross-linked AGEs increased significantly after BSA glycation. However, a notable decrease in the fluorescence intensity of CL, PEN, VL, and APN was observed upon treatment with AG and oak-derived active compounds **18**, **22**, and **23** for 24 h. Especially, AG and compounds **18** and **22** dramatically reduced the levels of these specific fluorescent AGEs even after 72 h of glycation. The results were

Table 1
Preliminary identification of the components from the different organs of three oak species by UPLC-Q-TOF-MS.

Type	No.	RT[a] (min)	[M–H]$^-$ (*m/z*)	Error (*ppm*)	Molecular Formula	MS Fragment	Phenolic class	Putative structure
I	**1**	1.23	191.0559	1.6	$C_7H_{12}O_6$		Phenolic acid	Quinic acid*
	2	3.08	169.0137	0.0	$C_7H_6O_5$		Phenolic acid	Gallic acid*
	3	3.38	343.0672	2.0	$C_{14}H_{16}O_{10}$	191.0559	Phenolic acid	Galloylquinic acid
	4	6.89	353.0899	7.4	$C_{16}H_{18}O_9$	191.0559	Phenolic acid	Neochlorogenic acid*
	5	8.86	337.0919	−1.2	$C_{16}H_{18}O_8$	119.0500, 163.0387, 191.0559	Phenolic acid	3-*O*-Coumaroylquinic acid*
	6	9.50	353.0899	−1.2	$C_{16}H_{18}O_9$	191.0559	Phenolic acid	Chlorogenic acid*
	7	12.15	337.0919	−1.2	$C_{16}H_{18}O_8$	191.0559	Phenolic acid	5-*O*-Coumaroylquinic acid*
	8	12.86	337.0919	−1.2	$C_{16}H_{18}O_8$	119.0500, 163.0387, 173.0458, 191.0559	Phenolic acid	4-*O*-Coumaroylquinic acid*
	9	16.78	515.1187	−0.6	$C_{25}H_{24}O_{12}$	173.0458, 179.0353, 191.0559	Phenolic acid	3,4-Dicaffeoylquinic acid*
	10	17.13	515.1187	−0.6	$C_{25}H_{24}O_{12}$	179.0353, 191.0559	Phenolic acid	3,5-Dicaffeoylquinic acid*
	11	18.02	515.1187	−0.6	$C_{25}H_{24}O_{12}$	173.0458, 179.0353, 191.0559	Phenolic acid	4,5-Dicaffeoylquinic acid*
II	**12**	3.23	783.0709	3.6	$C_{34}H_{24}O_{22}$	300.9988, 481.0636	Ellagitannin	Di-HHDP-glucose(pedunculagin) isomer I
	13	3.63	1101.0721	2.5	$C_{48}H_{30}O_{31}$	300.9988,	Ellagitannin	Valoneoyl-NHTP-glucose isomer I
	14	4.44	1101.0721	2.5	$C_{48}H_{30}O_{31}$	300.9988,	Ellagitannin	Valoneoyl-NHTP-glucose isomer I
	15	4.49	783.0709	3.6	$C_{34}H_{24}O_{22}$	300.9988, 481.0636	Ellagitannin	Di-HHDP-glucose(pedunculagin) isomer II
	16	4.85	933.0642	0.9	$C_{41}H_{26}O_{26}$	300.9988,	Ellagitannin	Vescalagin*
	17	5.35	783.0709	3.6	$C_{34}H_{24}O_{22}$	300.9988, 481.0636	Ellagitannin	Di-HHDP-glucose(pedunculagin) isomer III
	18	6.24	933.0642	0.9	$C_{41}H_{26}O_{26}$	300.9988, 631.0605	Ellagitannin	Castalagin*
	19	8.01	783.0709	3.6	$C_{34}H_{24}O_{22}$	300.9988, 481.0636	Ellagitannin	Di-HHDP-glucose(pedunculagin) isomer IV
	20	10.96	933.0642	0.9	$C_{41}H_{26}O_{26}$	300.9988,	Ellagitannin	Vescalagin/Castalagin isomer
	21	10.96	935.0810	2.0	$C_{41}H_{28}O_{26}$	300.9988, 633.0742	Ellagitannin	Casuarinin
	22	15.57	300.9988	1.3	$C_{14}H_6O_8$	300.9988	Ellagic acid	Ellagic acid*
III	**23**	8.36	577.1331	−2.6	$C_{30}H_{26}O_{12}$	289.0710, 407.0787	Flavan-3-ol	Procyanidin B1*
	24	8.61	577.1331	−2.6	$C_{30}H_{26}O_{12}$	289.0710, 407.0787	Flavan-3-ol	Procyanidin B-type isomer
	25	9.45	289.0710	−0.7	$C_{15}H_{14}O_6$		Flavan-3-ol	(+)-Catechin*
	26	12.46	289.0710	−0.7	$C_{15}H_{14}O_6$		Flavan-3-ol	(−)-Epicatechin*
	27	13.77	465.1031	−0.4	$C_{21}H_{22}O_{12}$	285.0424	Flavanonol	(2R,3R)-(+)-Glucodistylin*
	28	14.22	465.1031	−0.4	$C_{21}H_{22}O_{12}$	285.0424	Flavanonol	Taxifolin-*O*-hexoside
	29	14.43	465.1031	−0.4	$C_{21}H_{22}O_{12}$	285.0424	Flavanonol	(2S,3S)-(+)-Glucodistylin*
	30	14.83	479.0843	3.5	$C_{21}H_{20}O_{13}$	316.0212	Flavonol	Myricetin-*O*-hexoside
	31	15.01	479.0843	3.5	$C_{21}H_{20}O_{13}$	316.0212	Flavonol	Myricetin-*O*-hexoside
	32	15.46	465.1031	−0.4	$C_{21}H_{22}O_{12}$	285.0424	Flavanonol	Taxifolin-3′-*O*-glucopyranoside
	33	15.74	463.0884	1.5	$C_{21}H_{20}O_{12}$	316.0212	Flavonol	Myricitrin (myricetin-3-rhamnoside)*
	34	15.84	463.0884	1.5	$C_{21}H_{20}O_{12}$	301.0344, 300.0285	Flavonol	Hyperoside*
	35	16.00	463.0884	1.5	$C_{21}H_{20}O_{12}$	301.0344, 300.0285	Flavonol	Isoquercitrin*
	36	15.97	303.0512	2.3	$C_{15}H_{12}O_7$		Flavanonol	Taxifolin*
	37	16.58	433.0803	7.4	$C_{20}H_{18}O_{11}$	301.0344, 300.0285	Flavonol	Quercetin-3-*O*-alpha-L-arabinopyranoside*
	38	16.58	447.0947	4.5	$C_{21}H_{20}O_{11}$	285.0329	Flavonol	Kaempferol-*O*-hexoside
	39	16.85	433.0755	−3.7	$C_{20}H_{18}O_{11}$	301.0344, 300.0285	Flavonol	Avicularin*
	40	17.03	447.0947	4.5	$C_{21}H_{20}O_{11}$	285.0329	Flavonol	Astragalin*
	41	17.18	447.0947	4.5	$C_{21}H_{20}O_{11}$	301.0344, 300.0285	Flavonol	Quercitrin*
	42	17.28	477.1042	1.9	$C_{22}H_{22}O_{12}$	314.0422	Flavonol	Isorhamnetin-3-*O*-glucoside*
	43	22.54	301.0344	−1.3	$C_{15}H_{10}O_7$		Flavonol	Quercetin*
	44	23.15	593.1277	−3.0	$C_{30}H_{26}O_{13}$	285.0329, 447.0947	Flavonol	Tiliroside*
	45	25.95	285.0385	−4.9	$C_{15}H_{10}O_6$		Flavonol	Kaempferol*
IV	**46**	15.29	741.2628	3.0	$C_{34}H_{46}O_{18}$	417.1578, 579.2067, 787.2662	Lignans	Syringaresinol-di-*O*-glucoside*
	47	17.16	579.2067	−1.9	$C_{28}H_{36}O_{13}$	417.1578	Lignans	Syringaresinol-4-*O*-glucoside*

[a] Retention time (RT) of peaks in the UPLC-MS base peak intensity (BPI) chromatogram.
* Confirmed by a standard comparison.

further validated through emission fluorescence spectra at excitation wavelengths of 335 (for PEN and APN) and 370 nm (for CL and VL), as illustrated in Fig. 4C.

3.5. *Effect of the oak-derived components on protein glycoxidation*

The inhibitory effects of the oak-derived components on protein glycoxidation in the gBSA^{fru} model were also evaluated by measuring the fluorescence intensity of representative glycoxidation markers, including di-Tyr, NFK, and kynurenine. As shown in Fig. 4B, the levels of these three protein glycoxidation markers increased significantly after BSA glycation. However, a notable decrease in the fluorescence intensity of di-Tyr, NFK, and kynurenine was observed upon treatment with AG and oak-derived active compounds **18**, **22**, and **23** for 24 h. Especially, AG and compounds **18** and **22** significantly reduced the levels of these glycoxidation markers even after 72 h of glycation. The results were further validated through emission fluorescence spectra at excitation wavelengths of 335 (for di-Tyr and NFK) and 370 nm (for kynurenine), as illustrated in Fig. 4C.

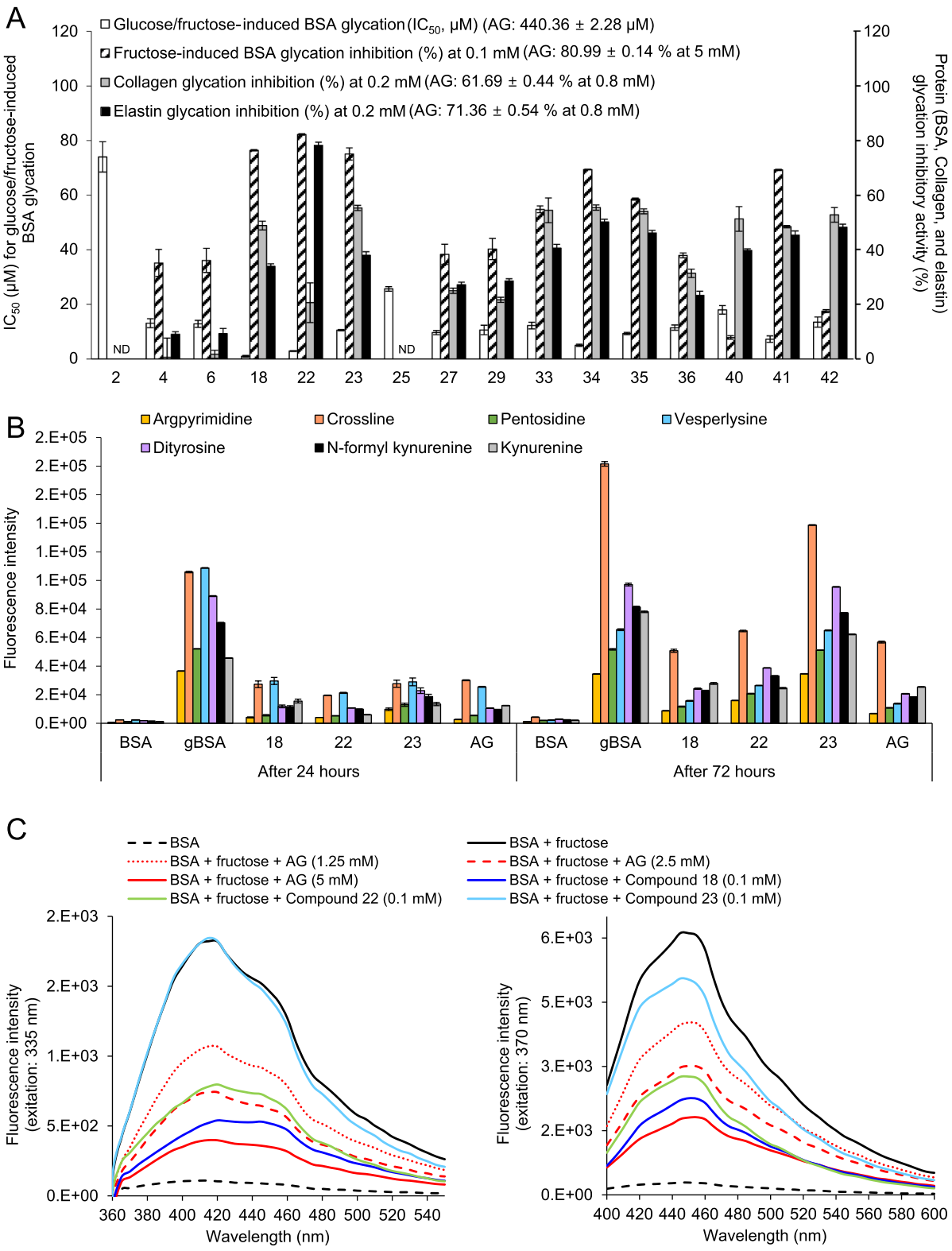

Fig. 4. Effects of oak-derived components and aminoguanidine (AG) on the formation of total fluorescent AGEs in the BSA-glucose/fructose model, the BSA + fructose ($gBSA^{fru}$) model, the collagen + glyceraldehyde model, and the elastin + glyceraldehyde model (A). Effects of the active compounds and AG on the formation of protein glycoxidation products and four specific fluorescent AGEs in the $gBSA^{fru}$ model (B). Fluorescence emission spectra of BSA, $gBSA^{fru}$, and $gBSA^{fru}$ + active components excited at 335 and 370 nm (C).

3.6. Inhibition of the oak-derived components on aggregation of β-amyloid fibrillation

Formation of β-amyloid fibrillation in the $gBSA^{fru}$ model was assessed using a ThT-labeled fluorescence assay (Bouma et al., 2003). Fig. 5A and B illustrate the fluorescence spectra and the inhibition rates of amyloid fibrillation in the $gBSA^{fru}$ model treated with oak-derived components, respectively. The fluorescence intensity in the $gBSA^{fru}$

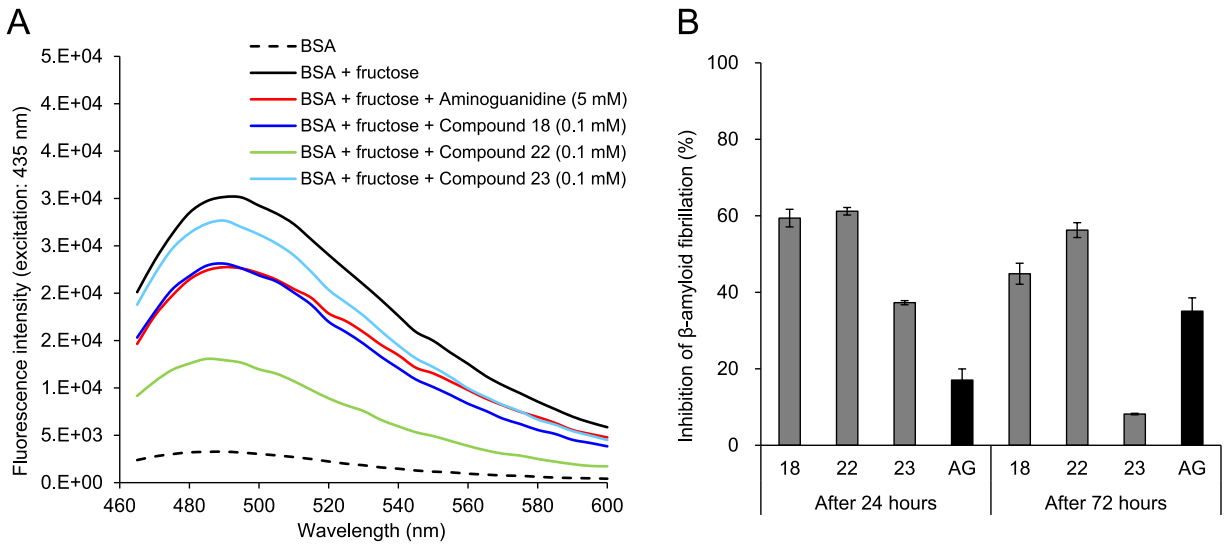

Fig. 5. The fluorescence spectra (A) and inhibition rates (B) of oak-derived components on the formation of β-amyloid fibrillation in the BSA-fructose model.

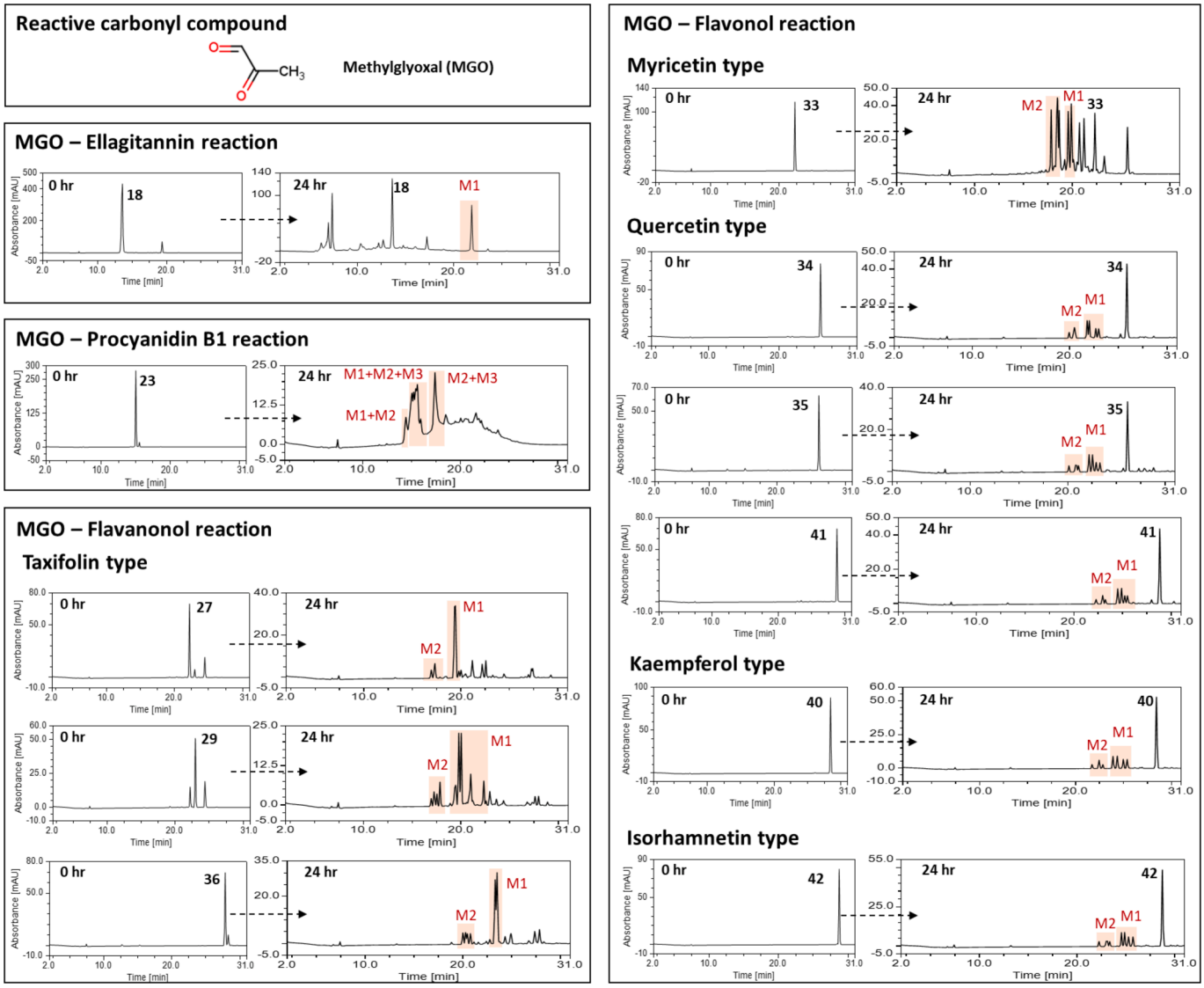

Fig. 6. The HPLC chromatogram of compounds after incubation with methylglyoxal (MGO) for 24 h (M1, MGO-compound adduct; M2, di-MGO-compound adduct; M3, tri-MGO-compound adduct).

model was signficantly higher than that of native BSA, indicating substantial aggregation of the produced AGEs with BSA and subsequent formation of cross-linked structures. In contrast, treatment with AG and oak-derived active compounds **18** and **22** significantly decreased BSA aggregation. As shown in Fig. 5B, compounds **18** and **22** at a concentration of 0.1 mM prevented 44.85 % and 56.27 % of amyloid-like fibril formation, respectively, surpassing the inhibition observed with AG (35.08 %).

3.7. MGO trapping capacities of the oak-derived compounds

The reaction mixture of MGO with anti-glycation active compounds from the three oak species at a 3:1 M ratio was analyzed using HPLC-ESI-Q-TOF-MS (Fig. 6 and Table 2). For the MGO-compound reaction mixture, several new peaks appeared in the HPLC chromatogram (Fig. 6). Based on the mass fragmentation patterns of the peaks generated after the reaction (Table 2), all the tested flavonoids (**23, 27, 29, 33–35, 40–42**) were shown to form MGO adducts, including mono-MGO adducts (M1) with an increase of 72 mass units ($C_3H_4O_2$) and di-MGO adducts (M2) with an increase of 144 mass units ($C_3H_4O_2 \times 2$). Interestingly, tri-MGO adducts (M3) with an increase of 216 mass units ($C_3H_4O_2 \times 3$) were detected in the MGO-procyanidin B1 (**23**) reaction mixture, together with mono- and di-MGO adducts. On the basis of the present results and previous studies (Li et al., 2014), unsubstituted carbons at flavonoid (C6- and C8-position of A-ring) or procyanidin (C6- and C8-position of A-ring, C6′-position of D-ring, and C4′-position of F-ring) scaffold were highly possible MGO trapping sites (Fig. 7).

Unlike flavonoids and procyanidin, castalagin (**18**), an ellagitannin, could trap MGO by binding mono-MGO to the degradation product rather than itself. For the MGO–compound **18** reaction mixture, new peaks appeared in the HPLC chromatogram after one day of incubation with MGO. Among them, a peak at the retention time (RT) of 7.02 min was observed to have the molecular formula of $C_{27}H_{19}O_{18}$ (*m/z* of 631.0596 $[M–H]^-$) with a fragment ion of *m/z* 300.9974, suggesting that this product is castalin. The peak at a RT of 21.87 min was observed to have a molecular formula of $C_{17}H_7O_{10}$ (*m/z* of 371.0044 $[M–H]^-$) with a fragment ion of *m/z* 300.9953 [ellagic acid–H]-, suggesting that this product is an ellagic acid-MGO (Fig. 6 and Table 2). Based on the fragmentation patterns of the peaks formed after the reaction, it was predicted that the HHDP moiety of castalagin (**18**) reacts with MGO and dissociates from the parent body to form M1 (Fig. 7). In contrast, caffeoylquinic acid (**4** and **6**) and ellagic acid (**22**) did not form adducts with MGO. Taken together, the HPLC-Q-TOF-MS analysis confirmed that flavonoids and ellagitannins derived from oaks formed mono-, di-, or tri-MGO adducts, thereby eliminating MGO, which is a reactive carbonyl intermediate and an important precursor of AGEs.

Table 2
MGO trapping capacities of the components from the different parts of three different oak species.

Compounds	Detected MGO–compound adducts $[M - H]^-$
Neochlorogenic acid (**4**)	*NA*
Chlorogenic acid (**6**)	*NA*
Castalagin (**18**)	371.0044 (M1)
Ellagic acid (**22**)	*NA*
Procyanidin B1 (**23**)	793.1993 (M3), 721.1783 (M2), 649.1534 (M1)
(2R,3R)-(+)-Glucodistylin (**27**)	609.1467 (M2), 537.1241 (M1)
(2S,3S)-(−)-Glucodistylin (**29**)	609.1467 (M2), 537.1241 (M1)
Myricitrin (**33**)	607.1320 (M2), 535.1113 (M1)
Hyperoside (**34**)	607.1320 (M2), 535.1113 (M1)
Isoquercitrin (**35**)	607.1320 (M2), 535.1113 (M1)
Taxifolin (**36**)	447.0956 (M2), 375.0742 (M1)
Astragalin (**40**)	591.1354 (M2), 519.1144 (M1)
Quercitrin (**41**)	591.1354 (M2), 519.1144 (M1)
Isorhamnetin-3-*O*-glucoside (**42**)	621.1455 (M2), 549.1252 (M1)

NA No adducts were detected.

4. Discussion

Herein, we investigated the antioxidant and anti-glycation effects of 70 % ethanolic and aqueous extracts of the three organs (leaves, twigs, and fruits) of the *Q. dentata*, *Q. serrata*, and *Q. aliena*. As a result, all tested extract except for 70 % ethanolic extract from the *Q. aliena* fruits showed strong radical ($ABTS^{\cdot+}$ and DPPH) scavenging activity as well as good inhibition against monosaccharide-induced AGE formation. In particular, the 70 % EtOH extracts of the leaves and twigs of *Q. aliena* demonstrated anti-glycation effects that were 1.5 to 2 times stronger than those of onion (*Allium cepa* L.) extract, which has been validated as an effective anti-glycation agent in several studies. Additionally, these extracts exhibited comparable antioxidant activity (Kim and Kim, 2003; Yang et al., 2018). Therefore, the overall phytochemical profile of the leaves, stems, and fruits from these active oak species was analyzed using UPLC-Q-TOF-MS. For MS analysis, MS^e acquisition mode was employed to obtain a full catalog of information for both precursor (low energy function) and fragment ions (high energy function) in a single analysis. The first, collected at low energy, yields accurate mass precursor ion spectra. The second, at high energy, yields the exact mass of the fragment ions. Based on the UPLC-ESI-Q-TOF-MS analysis, eleven phenolic acids (gallic acid and quinic acid derivatives), ellagic acid, ten ellagitannins, twenty-three flavonoid derivatives, and two lignans were identified. Interestingly, taxifolin and its glycosides were only detected in *Q. serrata*. In addition, the galloylquinic acid **(3)** and ellagitannins of the di-HHDP-glucose structure and galloyl-di-HHDP-glucose structure (casuarinin, **21**) were relatively high in *Q. aliena* when compared with the values for the other oak species.

Several studies have demonstrated that the phytochemicals found in oak species have antioxidant effects (Othón-Díaz et al., 2023). However, there has been little investigation into how they function in the glycation of diverse proteins and how they interact with a reactive carbonyl intermediate. Therefore, the active ingredients were systematically explored by confirming the ability of the main oak components to inhibit glycation of various proteins (BSA, collagen, and elastin).

Serum albumin glycation was induced by monosaccharides (glucose and fructose). Ellagic acid (**22**) and castalagin (**18**) showed notable effects, and flavonoid glycosides (quercetin > taxifolin > myricetin > isorhamnetin > kaempferol) and procyanidin B1 (**23**) showed strong inhibitory effects. Based on these results, it was confirmed that components with an ellagic acid-type structure can effectively inhibit BSA glycation and that the effect varies depending on the number of hydroxyl groups in the flavonoid.

Ellagic acid and ellagitannin are bioactive polyphenols commonly found in oak trees and are abundant in some fruits (almonds, pomegranates, and raspberries) (Landete, 2011). Ellagitannins are complex ellagic acid derivatives that are hydrolyzed by acids or bases to produce HHDP, which is then spontaneously lactonized to ellagic acid (Evtyugin et al., 2020). Ellagic acids and ellagitannins, similarly to other polyphenols, exhibit a variety of biological actions such as antioxidant, anti-estrogenic, and estrogenic effects, as well as prebiotic and anti-inflammatory activities, suggesting that they may be beneficial to human health (Larrosa et al., 2010; Sharifi-Rad et al., 2022). In our previous study, tellimagrandin II, the first ellagitannin formed from 1,2,3,4,6-penta-*O*-galloyl-glucose (PGG), exhibited strong inhibition of protein glycation by trapping RCCs and excellent binding ability to AGE receptors (RAGE) (Seong et al., 2023). Similarly, Ma et al. (2015) demonstrated that PGG inhibited early glycation by preventing sugar induced conformational changes of the protein (α-helix to β-sheet) via molecular docking simulations and matrix assisted laser desorption/ionization time of flight-TOF analysis (Ma et al., 2015). In line with these findings, the present study is the first to demonstrate the inhibitory effects of oak-derived ellagitannin, castalagin (**18**), against protein glycation.

During aging and for patients affected by diabetes, AGE accumulation has been detected in various tissues, including the glomerular

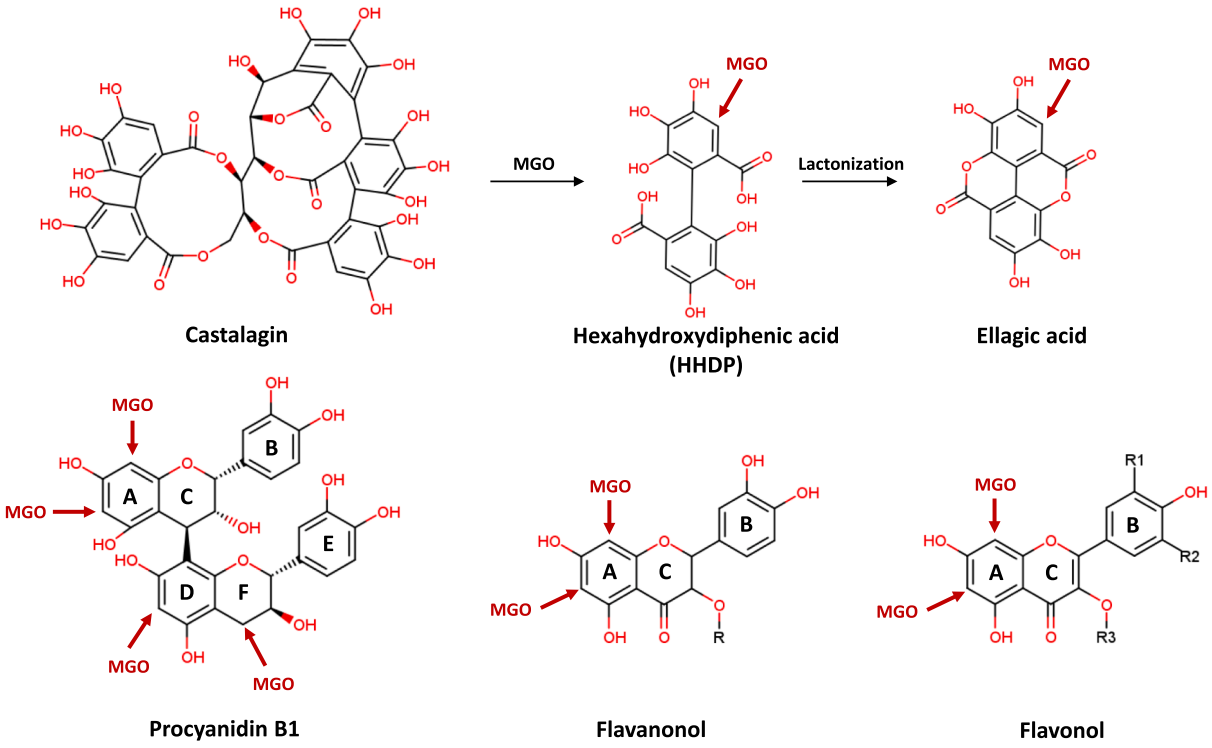

Fig. 7. Possible mechanism for production of MGO-compound adducts.

basement membrane, skeletal/smooth vascular muscle, elastin, and articular collagen (Gkogkolou and Böhm, 2012). Proteins with long biological half-lives, such as elastin and collagen, which have slow turnover rates of more than 10 years, are more prone to glycation and AGE generation than other proteins (Muir et al., 2021). Collagen and elastin are the major fibers that constitute the extracellular matrix (ECM). Elastin provides skin elasticity and collagen provides tensile strength. In particular, the skin collagen content was greater than 70 %, whereas that of elastin was approximately 2 % (Uitto, 1986). Collagen is not only employed as a mechanical support system for cells and tissues in the skin, but is also an active component capable of interacting with cells and influencing numerous cellular functions, such as proliferation, migration, and differentiation. During glycation, reducing sugar binds to the free lysine or arginine residues of elastin and collagen to form a Schiff base. The accumulation of cross-linked AGEs in skin proteins has various negative effects, including reduced solubility and flexibility of the collagen triple helix; decreased arterial/myocardial compliance; and increased vascular stiffness, diastolic function, and systolic hypertension (Gkogkolou and Böhm, 2012). In addition, skin elasticity declines with age, and this trend was more pronounced in patients with diabetes who experienced increased glycative stress (Yonei et al., 2010). Therefore, the anti-glycation potential of the active oak ingredients against two skin proteins (elastin and collagen) was evaluated. The glycation of these two skin proteins was induced by glycoaldehyde, which is an α-hydroxyaldehyde, and the anti-glycation potential was measured for active compounds at the same dose (0.2 mM). As a result, ellagic acid significantly inhibited elastin glycation, while having little to no impact on collagen glycation. In contrast, ellagitannins had a minimal impact on the glycation of elastin and a nearly 50 % inhibitory effect on the glycation of collagen. Furthermore, flavonoid glycosides, excluding taxifolin and its glycosides, inhibit collagen and elastin glycation by approximately 50 %. Recent studies have revealed that rutin, a representative quercetin rutinoside, is abundant in various foods, and its metabolites can effectively prevent AGE formation in glucose-induced collagen glycation (Cervantes-Laurean et al., 2006). In addition, Chang et al. reported that cranberry juice polyphenols, including procyanidins and quercetin, can effectively prevent MGO-induced collagen glycation and cross-linking (Chang et al., 2022). Urios and colleagues demonstrated that 3′-OH, 4-oxo, and delta$_{2\text{-}3}$ in the flavonoid scaffold are important for inhibitory activity against collagen glycation by measuring the formation of PEN, which is a specific marker of protein cross-link as well as glycoxidation, using HPLC (Urios et al., 2007). Taken together, it was proven that the flavonols are more effective than flavanonols at inhibiting the glycation of skin proteins and that the inhibitory effects increase alongside the number of hydroxyl groups linked to the B-ring of the flavonoids.

To elucidate the mechanism of action of the oak-derived active ingredients in inhibiting protein glycation, their effects on the middle- and end-stages of the protein glycation process were evaluated. MGO is the representative RCC generated during the middle-stage of the protein glycation. MGO influences the formation of AGEs and cross-linked aggregates in the later stages of protein glycation by covalently binding to functional groups of proteins and releasing free radicals (Chaudhuri et al., 2016). The MGO-trapping capacities of oak-derived active ingredients were assessed using HPLC-Q-TOF-MS. Several new peaks were observed in the HPLC chromatogram, which indicated that the active ingredients formed adducts with mono-, di-, and tri-MGO. The binding aspect of oak-derived active ingredients to MGO was confirmed by Q-TOF-MS analysis of the precursor ion spectrum and MS fragmentation pattern of the newly created MGO adduct using the low-energy and high-energy functions of the MS^{e} acquisition mode, respectively. In the MGO-catalagin (**18**) reaction mixture, mono-MGO was trapped by HHDP, which formed when the parent molecule (**18**) was broken, thus creating an adduct. For flavonoids (**23, 27, 29, 33–36, 40–42**), MGO molecules combined with the unsubstituted carbons (C6- and C8-positions) at the A-ring of the flavonoid to form mono- and di-MGO adducts. Interestingly, tri-MGO adducts were detected in the MGO-procyanidin B1 (**23**) reaction mixture, together with mono- and di-MGO adducts. However, because the ellagic acid (**22**) and caffeoylquinic acids (**4** and **6**) did not form adducts with MGO, further research on their other anti-glycation mechanisms should be conducted.

The generated advanced glycation end-products (AGEs) can lead to

intramolecular protein cross-linking, further promoting β-amyloid fibrillation associated with β-sheet formation during the later stages of protein glycation. These protein aggregations may impair both mechanical properties and biological functions (Zhang et al., 2022). Furthermore, the non-enzymatic glycation is accompanied by oxidation. During glycoxidation, tyrosine (Tyr) and tryptophan (Trp) residues are readily modified, resulting in the formation of fluorescent products. Particularly, Tyr residues are converted to kynurenine, while Trp residues are transformed into di-Tyr and NFK. Glycoxidation can also induce conformational changes in proteins, leading to the formation of amyloid fibrils (Eze and Tola, 2020). In the current study, castalagin (**18**) and ellagic acid (**22**) were found to inhibit the formation of cross-linked AGEs (CL, PEN, and VL), non-cross-linked AGEs (APN), and glycoxidation products (di-Tyr, NFK, and kynurenine) by measuring the fluorescence intensity and spectra at specific excitation and emission wavelengths of fluorescent AGEs and glycoxidation products generated from BSA glycation. Additionally, the glycated BSA solution, when incubated with ThT, exhibited increased fluorescence, indicating the presence of a β-sheeted conformation compared to the native BSA solution. However, castalagin (**18**) and ellagic acid (**22**) effectively reduced the ThT fluorescence intensity resulting from BSA glycation, demonstrating their strong potential to inhibit protein aggregation. Therefore, the potent inhibitory effects of the three oak species (*Q. dentata, Q. serrata,* and *Q. aliena)* on protein glycation appear to be due to the presence of ellagitannins and flavonoids, which possess inhibitory potential against protein glycation, glycoxidation, and aggregation, as well as RCC-trapping abilities.

5. Conclusions

The components of three oak species (*Q. dentata, Q. serrata, and Q. aliena)* were profiled, and their anti-glycation effects were systematically examined. This study is the first to demonstrate that castalagin (**18**), a major ellagitannin in oak, acts as an inhibitor of non-enzymatic protein (BSA, collagen, and elastin) glycation by trapping RCCs and inhibiting AGE production. In addition, the anti-glycation efficiency and RCC-trapping ability of the oak-derived flavonoids were examined, and a structure–activity correlation was established. Taken together, the results of our study might help deepen our understanding of the different oak components and aid in the development of functional foods and pharmaceuticals to manage various disorders caused by aging and excessive sugar consumption. Thus, the active ingredients in oak leaves, twigs, and fruits (mainly ellagitannins and flavonoid derivatives) are promising natural anti-glycation compounds with preventive and therapeutic potential against AGE-related disorders in multiple tissues.

CRediT authorship contribution statement

Su Hui Seong: Writing – review & editing, Writing – original draft, Methodology, Investigation, Formal analysis, Conceptualization. **Bo-Ram Kim:** Resources, Investigation. **Seahee Han:** Resources. **Jin-Ho Kim:** Formal analysis. **Sua Im:** Resources. **Tae-Su Kim:** Formal analysis. **Chan Seo:** Formal analysis. **Ha-Nul Lee:** Formal analysis. **Jung Eun Kim:** Resources. **Ji Min Jung:** Resources. **Myoung Lae Cho:** Resources, Conceptualization. **Kyung-Min Choi:** Supervision. **Jin-Woo Jeong:** Supervision, Project administration, Funding acquisition.

Funding

This work was supported by a grant from the Honam National Institute of Biological Resources (HNIBR), funded by the Ministry of Environment (MOE) of the Republic of Korea (HNIBR202302115), and the Korea Environment Industry & Technology Institute (KEITI) through a project aimed at advancing multi-ministerial national biological research resources, funded by the Korea Ministry of Environment (MOE) (RS-2023-00230402).

Declaration of competing interest

The authors declare that they have no known competing financial interests or personal relationships that could have appeared to influence the work reported in this paper.

References

Awasthi, S., Saraswathi, N.T., 2016. Carbonyl scavenging and chemical chaperon like function of essential amino acids attenuates non-enzymatic glycation of albumin. RSC Adv. 6 (29), 24557–24564. https://doi.org/10.1039/C5RA27460E.

Bouma, B., Kroon-Batenburg, L.M.J., Wu, Y.-P., Brünjes, B., Posthuma, G., Kranenburg, O., de Groot, P.G., Voest, E.E., Gebbink, M.F.B.G., 2003. Glycation induces formation of amyloid cross-β structure in albumin. J. Biol. Chem. 278 (43), 41810–41819. https://doi.org/10.1074/jbc.M303925200.

Burlacu, E., Nisca, A., Tanase, C., 2020. A comprehensive review of phytochemistry and biological activities of *Quercus* species. Forests 11 (9), 904. https://doi.org/10.3390/f11090904.

Cervantes-Laurean, D., Schramm, D.D., Jacobson, E.L., Halaweish, I., Bruckner, G.G., Boissonneault, G.A., 2006. Inhibition of advanced glycation end product formation on collagen by rutin and its metabolites. J. Nutr. Biochem. 17 (8), 531–540. https://doi.org/10.1016/j.jnutbio.2005.10.002.

Chang, H., Johnson, E., Khoo, C., Wang, W., Gu, L., 2022. Cranberry juice polyphenols inhibited the formation of advanced glycation end products in collagens, inhibited advanced glycation end product-induced collagen crosslinking, and cleaved the formed crosslinks. J. Agric. Food Chem. 70 (49), 15560–15569. https://doi.org/10.1021/acs.jafc.2c06502.

Chaudhuri, J., Bains, Y., Guha, S., Kahn, A., Hall, D., Bose, N., Gugliucci, A., Kapahi, P., 2018. The role of advanced glycation end products in aging and metabolic diseases: bridging association and causality. Cell Metab. 28 (3), 337–352. https://doi.org/10.1016/j.cmet.2018.08.014.

Choei, H., Sasaki, N., Takeuchi, M., Yoshida, T., Ukai, W., Yamagishi, S.-I., Kikuchi, S., Saito, T., 2004. Glyceraldehyde-derived advanced glycation end products in Alzheimer's disease. Acta Neuropathol. 108 (3), 189–193. https://doi.org/10.1007/s00401-004-0871-x.

Dudonné, S., Vitrac, X., Coutière, P., Woillez, M., Mérillon, J.-M., 2009. Comparative study of antioxidant properties and total phenolic content of 30 plant extracts of industrial interest using DPPH, ABTS, FRAP, SOD, and ORAC assays. J. Agric. Food Chem. 57 (5), 1768–1774. https://doi.org/10.1021/jf803011r.

Evtyugin, D.D., Magina, S., Evtuguin, D.V., 2020. Recent advances in the production and applications of ellagic acid and its derivatives. A Review. Molecules 25 (12), 2745. https://doi.org/10.3390/molecules25122745.

Eze, F. N., Tola, A. J., 2020. Protein glycation and oxidation inhibitory activity of *Centella asiatica* phenolics (CAP) in glucose-mediated bovine serum albumin glycoxidation. Food Chem., 332, 127302. 10.1016/j.foodchem.2020.127302.

Gkogkolou, P., Böhm, M., 2012. Advanced glycation end products. Dermatoendocrinology 4 (3), 259–270. https://doi.org/10.4161/derm.22028.

Grillo, M.A., Colombatto, S., 2008. Advanced glycation end-products (AGEs): involvement in aging and in neurodegenerative diseases. Amino Acids 35 (1), 29–36. https://doi.org/10.1007/s00726-007-0606-0.

Jia, W., Guo, A., Zhang, R., Shi, L., 2023. Mechanism of natural antioxidants regulating advanced glycosylation end products of Maillard reaction. Food Chem. 404, 134541. https://doi.org/10.1016/j.foodchem.2022.134541.

Kim, H.Y., Kim, K., 2003. Protein glycation inhibitory and antioxidative activities of some plant extracts in vitro. J. Agric. Food Chem. 51 (6), 1586–1591. https://doi.org/10.1021/jf020850t.

Landete, J.M., 2011. Ellagitannins, ellagic acid and their derived metabolites: A review about source, metabolism, functions and health. Food Res. Int. 44 (5), 1150–1160. https://doi.org/10.1016/j.foodres.2011.04.027.

Larrosa, M., García-Conesa, M.T., Espín, J.C., Tomás-Barberán, F.A., 2010. Ellagitannins, ellagic acid and vascular health. Mol. Aspects Med. 31 (6), 513–539. https://doi.org/10.1016/j.mam.2010.09.005.

Li, X., Zheng, T., Sang, S., Lv, L., 2014. Quercetin inhibits advanced glycation end product formation by trapping methylglyoxal and glyoxal. J. Agric. Food Chem. 62 (50), 12152–12158. https://doi.org/10.1021/jf504132x.

Liu, L., Liu, L., Xie, J., Shen, M., 2022. Formation mechanism of AGEs in Maillard reaction model systems containing ascorbic acid. Food Chem. 378, 132108. https://doi.org/10.1016/j.foodchem.2022.132108.

Ma, H., Liu, W., Frost, L., Wang, L., Kong, L., Dain, J.A., Seeram, N.P., 2015. The hydrolyzable gallotannin, penta-O-galloyl-β-D-glucopyranoside, inhibits the formation of advanced glycation endproducts by protecting protein structure. Mol. Biosyst. 11 (5), 1338–1347. https://doi.org/10.1039/C4MB00722K.

Mazumder, M.A.R., Hongsprabhas, P., Thottiam Vasudevan, R., 2019. In vitro and in vivo inhibition of maillard reaction products using amino acids, modified proteins, vitamins, and genistein: A review. J. Food Biochem. 43 (12), e13089. https://doi.org/10.1111/jfbc.13089.

Morales, D., 2021. Oak trees (*Quercus* spp.) as a source of extracts with biological activities: A narrative review. Trends Food Sci. Technol. 109, 116–125. https://doi.org/10.1016/j.tifs.2021.01.029.

Muir, R., Forbes, S., Birch, D.J.S., Vyshemirsky, V., Rolinski, O.J., 2021. Collagen glycation detected by its intrinsic fluorescence. J. Phys. Chem. B 125 (39), 11058–11066. https://doi.org/10.1021/acs.jpcb.1c05001.

Ni, M., Song, X., Pan, J., Gong, D., Zhang, G., 2021. Vitexin inhibits protein glycation through structural protection, methylglyoxal trapping, and alteration of glycation

site. J. Agric. Food Chem. 69 (8), 2462–2476. https://doi.org/10.1021/acs.jafc.0c08052.

Othón-Díaz, E.D., Fimbres-García, J.O., Flores-Sauceda, M., Silva-Espinoza, B.A., López-Martínez, L.X., Bernal-Mercado, A.T., Ayala-Zavala, J.F., 2023. Antioxidants in Oak (*Quercus* sp.): Potential application to reduce oxidative rancidity in foods. Antioxidants 12 (4), 861. https://doi.org/10.3390/antiox12040861.

Perrone, A., Giovino, A., Benny, J., Martinelli, F., 2020. Advanced glycation end products (AGEs): biochemistry, signaling, analytical methods, and epigenetic effects. Oxid. Med. Cell. Longev. 2020, 3818196. https://doi.org/10.1155/2020/3818196.

Seong, S.H., Jung, H.A., Choi, J.S., 2021. Discovery of flazin, an alkaloid isolated from cherry tomato juice, as a novel non-enzymatic protein glycation inhibitor via in vitro and in silico studies. J. Agric. Food Chem. 69 (12), 3647–3657. https://doi.org/10.1021/acs.jafc.0c07486.

Seong, S.H., Kim, B.-R., Park, J.-S., Jeong, D.Y., Kim, T.-S., Im, S., Jeong, J.-W., Cho, M. L., 2023. Phytochemical profiling of *Symplocos tanakana* Nakai and *S. sawafutagi* Nagam. leaf and identification of their antioxidant and anti-diabetic potential. J. Pharm. Biomed. Anal. 233, 115441. https://doi.org/10.1016/j.jpba.2023.115441.

Sharifi-Rad, J., Quispe, C., Castillo, C.M.S., Caroca, R., Lazo-Vélez, M.A., Antonyak, H., Polishchuk, A., Lysiuk, R., Oliinyk, P., De Masi, L., Bontempo, P., Martorell, M., Daştan, S.D., Rigano, D., Wink, M., Cho, W.C., 2022. Ellagic acid: A review on its natural sources, chemical stability, and therapeutic potential. Oxid. Med. Cell. Longev. 2022, 3848084. https://doi.org/10.1155/2022/3848084.

Taïb, M., Rezzak, Y., Bouyazza, L., Lyoussi, B., 2020. Medicinal uses, phytochemistry, and pharmacological activities of *Quercus* species. Evid. Based Complement. Alternat. Med. 2020, 1920683. https://doi.org/10.1155/2020/1920683.

Takeuchi, M., Bucala, R., Suzuki, T., Ohkubo, T., Yamazaki, M., Koike, T., Kameda, Y., Makita, Z., 2000. Neurotoxicity of advanced glycation end-products for cultured cortical neurons. J. Neuropathol. Exp. Neurol. 59 (12), 1094–1105. https://doi.org/10.1093/jnen/59.12.1094.

Thornalley, P.J., 2003. Use of aminoguanidine (Pimagedine) to prevent the formation of advanced glycation endproducts. Arch. Biochem. Biophys. 419 (1), 31–40. https://doi.org/10.1016/j.abb.2003.08.013.

Uitto, J., 1986. Connective tissue biochemistry of the aging dermis: Age-related alterations in collagen and elastin. Dermatol. Clin. 4 (3), 433–446. https://doi.org/10.1016/S0733-8635(18)30806-4.

Urios, P., Grigorova-Borsos, A.-M., Sternberg, M., 2007. Flavonoids inhibit the formation of the cross-linking AGE pentosidine in collagen incubated with glucose, according to their structure. Eur. J. Nutr. 46 (3), 139–146. https://doi.org/10.1007/s00394-007-0644-0.

Vinson, J.A., Howard, T.B., 1996. Inhibition of protein glycation and advanced glycation end products by ascorbic acid and other vitamins and nutrients. J. Nutr. Biochem. 7 (12), 659–663. https://doi.org/10.1016/S0955-2863(96)00128-3.

Yamaguchi, F., Ariga, T., Yoshimura, Y., Nakazawa, H., 2000. Antioxidative and anti-glycation activity of garcinol from *Garcinia indica* fruit rind. J. Agric. Food Chem. 48 (2), 180–185. https://doi.org/10.1021/jf990845y.

Yang, S.J., Paudel, P., Shrestha, S., Seong, S.H., Jung, H.A., Choi, J.S., 2018. In vitro protein tyrosine phosphatase 1B inhibition and antioxidant property of different onion peel cultivars: A comparative study. Food Sci. Nutr. 7 (1), 205–215. https://doi.org/10.1002/fsn3.863.

Yin, P., Yang, L., Xue, Q., Yu, M., Yao, F., Sun, L., Liu, Y., 2018. Identification and inhibitory activities of ellagic acid- and kaempferol-derivatives from Mongolian oak cups against α-glucosidase, α-amylase and protein glycation linked to type II diabetes and its complications and their influence on HepG2 cells' viability. Arab. J. Chem. 11 (8), 1247–1259. https://doi.org/10.1016/j.arabjc.2017.10.002.

Yonei, Y., Miyazaki, R., Takahashi, Y., Takahashi, H., Nomoto, K., Yagi, M., Kawai, H., Kubo, M., Matsuura, N., 2010. Anti-glycation effect of mixed herbal extract in individuals with pre-diabetes mellitus. Anti Aging Med. 7 (5), 26–35. https://doi.org/10.3793/jaam.7.26.

Zhang, Y., Pan, Y., Li, J., Zhang, Z., He, Y., Yang, H., Zhou, P., 2022. Inhibition on α-glucosidase activity and non-enzymatic glycation by an anti-oxidative proteoglycan from *Ganoderma lucidum*. Molecules 27 (5), 1457. https://doi.org/10.3390/molecules2705145.